

Possible phase diagram of Helium 4

Jinwu Ye

Department of Physics, The Pennsylvania State University, University Park, PA, 16802
(August 26, 2019)

The phase diagram of He4 was previously thought to consist of only 3 phases: normal liquid, superfluid and normal solid. However, recent torsional oscillator experiments detected some signatures of a possible new state of matter: supersolid state which has both crystalline and superfluid order. Here, we develop a simple Quantum Ginsburg Landau theory to study all the possible phases in He4 from a unified point of view. This theory naturally and consistently leads to the existence of the supersolid. We use the theory to map out the global phase diagram of He4, explain several important experimental facts and also make some predictions that are amenable to experimental tests. A key prediction is that the X-ray scattering intensity from the SS ought to have an additional modulation *shifted* from that of the NS. The modulation amplitude is proportional to the Non-Classical Rotational-Inertial (NCRI) observed in the torsional oscillator experiments.

1. Introduction: A solid can not flow. While a superfluid can flow without any resistance. A supersolid (SS) is a new state of matter which has both the solid and superfluid order. The possibility of a supersolid phase in He4 due to very large zero point quantum fluctuations was theoretically speculated in 1970 [1–4]. Over the last 35 years, a number of experiments have been designed to search for the supersolid state without success. However, recently, by using torsional oscillator measurement, a PSU group lead by Chan observed a marked $1 \sim 2\%$ Non-Classical Rotational Inertial (NCRI) of solid He4 at $\sim 0.2K$, both when embedded in Vycor glass [5] and in bulk He4 [6]. The NCRI is a low temperature reduction in the rotational moment of inertia due to the superfluid component of solid He4 [3]. Some of the important experimental facts are: (1) the superfluid fraction has a non-monotonic dependence on the pressure, it increases first, reaches a maximum at $\sim 55 \text{ bar}$, then decreases to zero at a much higher pressure $p_u \sim 170 \text{ bar}$ [9]. (2) The supersolid has a very low critical velocity corresponding to $\sim 1 - 3$ flux quanta above which the NCRI is reduced (3) A tiny fraction of He^3 will decrease the superfluid fractions, but increases the supersolid to normal solid transition temperature considerably [9]. (4) The group also discovered 10^{-4} percent of superfluid density in solid hydrogen [11], even the 3d superfluid state of hydrogen is still elusive. They mapped out the experimental global phase diagram of He4 in the Fig.4 in [6]

The PSU experiments rekindled great theoretical interests in the still controversial supersolid phase of He4. There are two kinds of complementary theoretical approaches. The first is the microscopic numerical simulation [7]. The second is the phenomenological approach [8]. In this paper, we will address the following two questions from the second approach: (1) How can a supersolid phase naturally sneak into the the previously thought He4 phase diagram (2) if it does, what is the properties of the supersolid to be tested by experiments. Unfortunately, if a supersolid indeed happens as a ground state in He4 is beyond the scope of any phenomenological ap-

proach, very likely, of any theoretical approach. In this paper, we develop a simple and powerful quantum Ginsburg Landau (QGL) theory to map out the He4 phase diagram and study all the phases and phase transitions in a unified framework. The SS phase naturally and consistently fits into the phase diagram. The theory can be used to explain several important phenomena observed in the PSU experiments and also make sharp predictions to be tested by possible future experiments, especially X-ray scattering experiments in the SS state.

2. Ginsburg-Landau theory of He4: Let's start by reviewing all the known phases in He4. The density of a normal solid (NS) is defined as $n(\vec{x}) = n_0 + \sum_{\vec{G}} n_{\vec{G}} e^{i\vec{G}\cdot\vec{x}}$ where $n_{\vec{G}}^* = n_{-\vec{G}}$ and \vec{G} is any non-zero reciprocal lattice vector. In a normal liquid (NL), if the static liquid structure factor $S(k)$ has its first maximum peak at \vec{k}_n , then near $k = k_n$, $S^{-1}(k) \sim r_n + c(k^2 - k_n^2)^2$. If the liquid-solid transition is weakly first order, it is known that the classical free energy to describe the NL-NS transition is [13]:

$$f_n = \sum_{\vec{G}} \frac{1}{2} r_{\vec{G}} |n_{\vec{G}}|^2 - w \sum_{\vec{G}_1, \vec{G}_2, \vec{G}_3} n_{\vec{G}_1} n_{\vec{G}_2} n_{\vec{G}_3} \delta_{\vec{G}_1 + \vec{G}_2 + \vec{G}_3, 0} + u \sum_{\vec{G}_1, \vec{G}_2, \vec{G}_3, \vec{G}_4} n_{\vec{G}_1} n_{\vec{G}_2} n_{\vec{G}_3} n_{\vec{G}_4} \delta_{\vec{G}_1 + \vec{G}_2 + \vec{G}_3 + \vec{G}_4, 0} + \dots \quad (1)$$

where $r_{\vec{G}} = r_n + c(G^2 - k_n^2)^2$ is the tuning parameter controlled by the pressure.

It was known that the Superfluid (SF) to Normal Liquid transition at finite temperature is a 3d XY transition described by:

$$f_\psi = K |\nabla\psi|^2 + t |\psi|^2 + u |\psi|^4 + \dots \quad (2)$$

where ψ is the complex order parameter and t is the tuning parameter controlled by the temperature.

The coupling between $n(\vec{x})$ and $\psi(\vec{x})$ consistent with all the symmetry can be written down as:

$$f_{int} = v_1 n(\vec{x}) |\psi(\vec{x})|^2 + v_2 n^2(\vec{x}) |\psi(\vec{x})|^2 + \dots \quad (3)$$

where it is expected that the interactions are repulsive $v_1, v_2 > 0$. As shown in section 5, these repulsive interactions are crucial to shift down the supersolid transition temperature in Fig.1.

A NS is defined by $n_{\vec{G}} \neq 0, \langle \psi \rangle = 0$, while a supersolid (SS) is defined by $n_{\vec{G}} \neq 0, \langle \psi \rangle \neq 0$. From the NL side, one can approach both the NS and the SF. Inside the NL, $t > 0$, ψ has a gap, so can be integrated out, we recover the NS-NL transition tuned by $r_{\vec{G}}$ in Eqn.1 (Fig.1). Inside the NL $\langle n(\vec{x}) \rangle = n_0$, so we can set $n_{\vec{G}} = 0$ for $\vec{G} \neq 0$ in Eqn.3, then we recover the NL to SF transition tuned by t in Eqn.2 (Fig.1).

Although the NL-NS and NL-SF transitions are well understood, the SF-NS transition has not been investigated seriously. This transition must be in a completely different universality class than the NL-NS transition, because both sides break two completely different symmetry: internal global $U(1)$ symmetry and translational (and orientational) symmetry. It is certainly possible that the solid reached from the SF side is a new kind of solid than the NS reached from the NL side. In the following, incorporating quantum fluctuations into f_ψ (see Eqn.4) and considering the density-density coupling between ψ and n sector in Eqn.3, we will determine the global phase diagram of He4.

3. Two-component QGL theory in the ψ sector: In this section, we develop a two-component QGL theory in the ψ sector to replace Eqn.2 to describe the superfluid side of He4. The superfluid is described by a complex order parameter ψ whose *condensation* leads to the Landau's quasi-particles. Although the bare He4 atoms are strongly interacting, the Landau's quasi-particles are weakly interacting. The dispersion curve of superfluid state is shown in Fig. 1 b which has both a phonon sector and a roton sector. In order to focus on the low energy modes, we divide the spectrum into two regimes: the low momenta regime $k < \Lambda$ where there are phonon excitations with linear dispersion and high momentum regime $|k - k_r| < \Lambda \ll k_r$ where there is a roton minimum at the roton surface $k = k_r$. We separate the complex order parameters $\psi(\vec{x}, \tau) = \psi_1(\vec{x}, \tau) + \psi_2(\vec{x}, \tau)$ into $\psi_1(\vec{x}, \tau) = \int_0^\Lambda \frac{d^d k}{(2\pi)^d} e^{i\vec{k}\cdot\vec{x}} \psi(\vec{k}, \tau)$ and $\psi_2(\vec{x}, \tau) = \int_{|k-k_r|<\Lambda} \frac{d^d k}{(2\pi)^d} e^{i\vec{k}\cdot\vec{x}} \psi(\vec{k}, \tau)$ which stand for low energy modes near the origin and k_r respectively. For the notation simplicity, in the following, \int_Λ means $\int_{|k-k_r|<\Lambda}$. The QGL action in the ψ sector in the (\vec{k}, ω) space becomes:

$$\begin{aligned} \mathcal{S}_\psi = & \frac{1}{2} \int_0^\Lambda \frac{d^d k}{(2\pi)^d} \frac{1}{\beta} \sum_{i\omega_n} (\kappa\omega_n^2 + t + Kk^2) |\psi_1(\vec{k}, i\omega_n)|^2 \\ & + \frac{1}{2} \int_\Lambda \frac{d^d k}{(2\pi)^d} \frac{1}{\beta} \sum_{i\omega_n} (\kappa\omega_n^2 + \Delta_r + v_r(k - k_r)^2) |\psi_2(\vec{k}, i\omega_n)|^2 \\ & + u \int d^d x d\tau |\psi_1(\vec{x}, \tau) + \psi_2(\vec{x}, \tau)|^4 + \dots \end{aligned} \quad (4)$$

where $t \sim T - T_c$ where $T_c \sim 2.17K$ is the critical temperature of SF to NL transition at $p = 0.05 \text{ bar}$ and $\Delta_r \sim p_c - p$ where $p_c \sim 25 \text{ bar}$ is the critical pressure of SF to the SS transition at $T = 0$.

4. SF to SS transition and global phase diagram: In the SF state, the Feymann relation between the Landau quasi-particle dispersion relation in the ψ sector and the static structure factor in the n sector holds:

$$\omega(q) = \frac{q^2}{2mS(q)} \quad (5)$$

In the $q \rightarrow 0$ limit, $S(q) \sim q$, $\omega(q) \sim q$ recovers the ψ_1 sector near $q = 0$. The first maximum peak in $S(q)$ corresponds to the roton minimum in $\omega(q)$ in the ψ_2 sector, namely, $k_n = k_r$. As one increases the pressure p , the interaction u also gets bigger and bigger, the roton minimum Δ_r gets smaller and smaller. From Eqn.1 and Eqn.4, we can see that n and ψ_2 have very similar propagators. Because in the effective GL theory, we have to treat n and ψ on the same footing, so the lattice formation in n sector with $n(x) = \sum_{\vec{G}} n_{\vec{G}} e^{i\vec{G}\cdot\vec{x}}$ and density wave formation in ψ_2 sector with $\langle \psi_2(\vec{x}) \rangle = e^{i\theta_2} \sum_{m=1}^P \Delta_m e^{i\vec{Q}_m\cdot\vec{x}}$ where $Q_m = k_r$ may happen simultaneously. From Hansen-Verlet criterion [13], when $S(k_0)/n_0$ is sufficiently large, solidification in the n sector occurs, so the roton minimum remains *finite* just before its condensation. The repulsive ρ density- n density coupling in Eqn.3 $v_1 > 0$ simply shifts the DW by suitable constants along the three unit vectors in the direct lattice. These constants will be determined in the next section for different n lattices. Namely, the SS state consists of two inter-penetrating lattices formed by the n lattice and the ψ_2 density wave. Note that in a carefully prepared super-pressured sample, the roton minimum survives up to as high pressure as $p_r \sim 120 \text{ bar}$ [12]. Strikingly, this pressure $p_r \sim 120 \text{ bar}$ is close to $p_u \sim 170 \text{ bar}$ where the NCRI was extrapolated to vanish in the PSU's experiments [9]. These facts suggest the roton minimum in the meta-stable state in a super-pressured sample is replaced by a DW which is commensurate with the n lattice in the stable SS state.

Combining the roton condensation picture in this section with the results in section 2, we can sketch the following global phase diagram of He4.

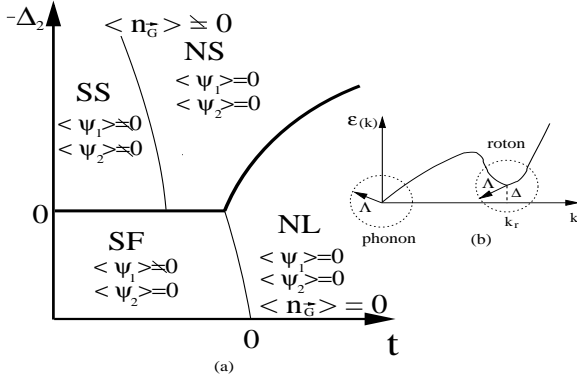


Fig.1: (a) The theoretical phase diagram of QGL model Eqn.4 in the pressure P versus the temperature T . T controls thermal fluctuations, while P tunes quantum fluctuations. Thick (thin) lines are 1st (2nd) order transitions. The critical temperatures of NL to SF and NS to SS transitions drop slightly as the pressure p increases because of the quantum fluctuations. (b) The separation of low (phonon) and high (roton) momenta regime in the SF.

5. The NS to SS transition: In this section, we approach the SS phase from the NS side and confirm it indeed exists and determine its lattice structure. In the NL, the BEC happens in the ψ_1 sector at $k = 0$, ψ_2 has a large gap and can be simply integrated out. In the NS, ψ stands for both tunneling process of He4 atoms due to large zero point quantum fluctuations. Due to the lack of particle-hole symmetry in the NS [3,2], there may be more vacancies than interstitials, an additional term $\psi_1 \partial_\tau \psi_1 + \psi_2 \partial_\tau \psi_2$ should exist and is very important at zero temperature and will be investigated in [14]. However, in the classical phase transitions investigated in this paper, this term can still be neglected, so the results should apply to both commensurate and incommensurate NS's. Due to the n lattice formation, the mass of ψ_1 was increased to $t_{\psi_1}^{NS} = t + v_1^{NS} n_0 + v_2^{NS} n_0^2 + v_2^{NS} \sum_{\vec{G}} |n_{\vec{G}}|^2 > t_{\psi_1}^{NL} = t + v_1^{NL} n_0 + v_2^{NL} n_0^2$, because we expect $v_1^{NS} > v_1^{NL} > 0, v_2^{NS} > v_2^{NL} > 0$. So the transition temperature T_{SS} from the NS to the SS will *shift down* to lower temperature $T_{SS} < T_c$ as shown in Fig.1. In the presence of the periodic potential of $n(x)$ lattice, ψ will form a Bloch wave, the u self-interaction in the ψ sector in Eqn.4 will certainly favor extended Bloch wave over strongly localized Wannier state. In principle, a full energy band calculation incorporating the interaction u is necessary to get the energy bands of ψ . Fortunately, qualitatively physical picture can be achieved without such a detailed energy band calculation. In the following, substituting the DW ansatz $\langle \psi_1(\vec{x}) \rangle = ae^{i\theta_1}$ and $\langle \psi_2(\vec{x}) \rangle = e^{i\theta_2} \sum_{m=1}^P \Delta_m e^{i\vec{Q}_m \cdot \vec{x}}$ where $Q_m = Q$ into Eqn.3, we study the effects of n lattice on $\psi = \psi_1 + \psi_2$. In order to get the lowest energy ground state, we must consider the following 4 conditions: (1) because any complex ψ (up to a global phase) will lead to local supercurrents which is costly, we can also take ψ to be real,

so \vec{Q}_m have to be paired as anti-nodal points. P has to be even (2) as shown from the Feymann relation Eqn.5, $\vec{Q}_m, m = 1, \dots, P$ are simply P shortest reciprocal lattice vectors, then translational symmetry of the lattice dictates that $\epsilon(\vec{K} = 0) = \epsilon(\vec{K} = \vec{Q}_m)$, ψ_1 and ψ_2 have to condense at the same time. (3) The point group symmetry of the lattice dictates $\Delta_m = \Delta$ and is real (4) The strong repulsive interaction $v_1 > 0$ favors $\psi(x=0) = 0$, so the Superfluid Density Wave (SDW) $\rho = |\psi|^2$ can avoid the n lattice as much as possible [15]. It turns out that the 4 conditions can fix the relative phase and magnitude of ψ_1 and ψ_2 to be $\theta_2 = \theta_1 + \pi, \Delta = a/P$, namely, $\psi = ae^{i\theta} (1 - \frac{2}{P} \sum_{m=1}^{P/2} \cos \vec{Q}_m \cdot \vec{x})$. In this state, the crystal momentum $\vec{k} = 0$ and the Fourier components are $\psi(\vec{K} = 0) = a, \psi(\vec{K} = \vec{Q}_m) = -a/P$ which oscillate in sign and decay in magnitude. In principle, higher Fourier components may also exist, but they decay very rapidly, so can be neglected without affecting the physics qualitatively. In the following, we will discuss 3 common close packed lattices *fcc, bcc, hcp* lattices respectively.

(a) $P = 8$: $\vec{Q}_i, i = 1, \dots, 8$ form the 8 shortest reciprocal lattice vectors generating a *bcc* reciprocal lattice which corresponds to a *fcc* direct lattice. The field is $\psi(\vec{x}) = a[1 - \frac{1}{4}(\cos \vec{Q}_1 \cdot \vec{x} + \cos \vec{Q}_2 \cdot \vec{x} + \cos \vec{Q}_3 \cdot \vec{x} + \cos \vec{Q}_4 \cdot \vec{x})]$. The local superfluid density $\rho_{DW}^l = |\psi(\vec{x})|^2$. The maxima of the DW $\psi_{max} = 2a$ appear in all the edge centers such as $(1/2, 0, 0)$ etc. and the centers of any cube such as $(1/2, 1/2, 1/2)$.

(b) $P = 12$: $\vec{Q}_i, i = 1, \dots, 12$ form the 12 shortest reciprocal lattice vectors generating a *fcc* reciprocal lattice which corresponds to a *bcc* direct lattice. The field is $\psi(\vec{x}) = a[1 - \frac{1}{6}(\cos \vec{Q}_1 \cdot \vec{x} + \cos \vec{Q}_2 \cdot \vec{x} + \cos \vec{Q}_3 \cdot \vec{x} + \cos \vec{Q}_4 \cdot \vec{x} + \cos \vec{Q}_5 \cdot \vec{x} + \cos \vec{Q}_6 \cdot \vec{x})]$. The maxima of the DW $\psi_{max} = 4/3a$ appear along any square surrounding the center of the cube such as $(1/2, \beta, 0)$ or $(1/2, 0, \gamma)$ etc. Note that He4 in Vycor glass takes a *bcc* lattice

(c) Unfortunately, a spherical $k_r = Q$ surface can not lead to lattices with *different* lengths of primitive reciprocal lattice vectors such as a *hcp* lattice. This is similar to the classical liquid-solid transition described by Eqn.1 where a single maximum peak in the static structure factor can not lead to a *hcp* lattice [13]. Here we can simply take the experimental fact that n forms a *hcp* lattice without knowing how to produce such a lattice from a GL theory Eqn.1. Because for an idea *hcp* lattice $c/a = \sqrt{8/3}$, an *hcp* lattice has 12 nearest neighbours, so its local environment may resemble that of an *fcc* lattice. We expect the physics (except the weak anisotropy of NCRI in the *hcp* lattice to be discussed in the following) is qualitatively the same as that in *fcc* direct lattice.

The results achieved in this section indeed confirm Fig.1 achieved from the roton condensation picture in the last section. An immediate prediction of our theory is that the X-ray scattering intensity from the SS has an additional modulation *shifted* from that of the NS. The

modulation amplitude is proportional to the maxima of the superfluid density $\rho_s^{max} \sim a^2$ which is the same as the NCRI observed in the PSU's torsional oscillator experiments. Unfortunately, so far, the X-ray scattering data is limited to high temperature $T > 0.8K > T_{SS}$ [16]. X-ray scattering experiments on lower temperature $T < T_{SS}$ are needed to test this prediction.

6. The NCRI and vortices in the SS: In the SS state, the $n(x)$ forms a normal lattice, at the same time, the unstable roton part is replaced by a stable DW formation commensurate with the underlying n lattice. Obviously, the $n(x)$ normal lattice takes away the vast majority of density from the superfluid density even at $T = 0$. The calculations in [14] showed that the total superfluid density in SS phase is $\rho_{ij}^{SS} \sim \rho_1 \delta_{ij} + \rho_{2ij} \sim Ka^2 \delta_{ij} + v_r \sum_{m=1}^P |\Delta_m|^2 Q_{mi} Q_{mj} / Q^2$ where $\Delta_m = a/P$. Because P is quite large, the second term is small, the anisotropy is weak for hcp lattice.

Obviously, in the sectors of ψ , there are also topological defects in the phase winding of θ which are vortices. At $T \ll T_{SS}$, the vortices can only appear in tightly bound pairs. However, as $T \rightarrow T_{SS}^-$, the vortices start to become liberated, this process renders the total NCRI to vanish above $T > T_{SS}$ in the NS state. In the SF phase, a single vortex energy costs a lot of energy $E_v^{SF} = \frac{\rho_s^{SF} h^2}{4\pi m^2} \ln \frac{R}{\xi_{SF}}$ where m is the mass of He atom, R is the system size and $\xi_{SF} \sim a$ is the core size of the vortex. This energy determines the critical velocity in SF $v_c^{SF} > 30cm/s$. In the SS state, because in the center of the SS vortex core, $\psi = 0$, so the vortices prefer to sit on one lattice site of the n lattice. Because the long distance behavior of SS is more or less the same as SF, we can estimate its energy $E_v^{SS} = \frac{\rho_s^{SS} h^2}{4\pi m^2} \ln \frac{R}{\xi_{SS}}$ [17]. We expect the core size of a supersolid vortex $\xi_{SS} \sim 1/\Lambda \gg 1/k_r \sim a \sim \xi_{SF}$. so inside the SS vortex core, we should also see the lattice structure of n . It is interesting to see if neutron or light scattering experiments can test this prediction. Compared to E_v^{SF} , there are two reductions, one is the superfluid density, another is the increase of the vortex core size $\xi_{SS} \gg \xi_{SF}$. These two factors contribute to the very low critical velocity $v_c^{SS} \sim 30\mu m/s < 10^{-3} v_c^{SF}$ where we find $\xi_{SS} > 2 \times 10^4 \xi_{SF}$.

7. Discussions on PSU's experiments: Although the NS to SS transition is in the same universality class as the NL to SF one, it may have quite different off-critical behaviours due to the DW structure in the SS state. In this section, we use this fact to address several experimental observations. We comment the effects of He3 impurities, assuming their diffusion process is slow. In the PSU experiments, the concentration x of He3 could be controlled in the range $40ppB < x < 200ppM$ [9]. At $x = 0.3ppM$, the average distance d_{imp} between the He3 impurities is $\sim 450\text{\AA}$ which is about 130 lattice constant. There are three widely separated length scales in this problem, $\xi_{SS} \gg d_{imp} \gg \xi_{SF}$. Although the

He3 impurity concentration is very dilute compared to $\xi_{SF} \sim a \sim 3.57\text{\AA}$, it is sufficiently dense compared to ξ_{SS} , so inside just one SS vortex core there are many He3 impurities. Slightly below T_{SS} , the number of vortex pairs are even less than that of He3 impurities, the SS is in the dilute vortex limit where the unbinding transition temperature T_{SS} is determined by the pinning due to impurities instead of by the logarithmic interactions between the vortices which is proportional to the superfluid stiffness. So the He3 impurities effectively pin the vortices and raise the unbinding critical temperature T_{SS} . On the other hand, He3 impurities will certainly decrease the superfluid density in both the ψ_1 and ψ_2 sector just like He3 impurities decreases superfluid density in the He4 superfluid. Note that in SF, slightly below T_{XY} , the number of vortex pairs are much larger than that of He3 impurities, the SF is in the dense vortex limit where the unbinding transition temperature T_{XY} is determined by the logarithmic interactions between the vortices which is also proportional to the superfluid stiffness. So in the SF, the He3 impurities hurt superfluid density which, in turn, lead to the reduction in T_{XY} .

In principle, in clean system, the specific heat measurement should show the λ peak as the NL to SF transition. We can also estimates the critical regime from the Ginsburg Criterion $t_G^{-1} \sim \xi_{SS}^3 \Delta C$ where ΔC is the specific jump in the mean field theory. Because of the cubic dependence on ξ_{SS} , large ξ_{SS} leads to extremely narrow critical regime. It will be very difficult to observe the λ peak around T_{SS} . So the 3D XY critical behavior is essentially irrelevant, instead mean field Gaussian theory should apply. The mean field jump will certainly be smeared by the presence of He3 impurities. So we expect that the λ peak will be smeared in the specific heat measurement near $T = T_{SS}$. We conclude that the smearing of specific heat anomaly in the presence of He3 impurities is closely related to the opposite trend of the dependence of T_{SS} and the superfluid density on the concentration of He3 impurities.

8. Conclusions: The QGL theory developed in this paper leads to a global and unified picture of He4 physics at any temperature and pressure. We investigate the SS state from both the SF and the NS side and find completely consistent description of the properties of the SS state. We found that the SF to the SS transition is a first order transition driven by the collapsing of roton minimum in the SF side, while the NS to SS transition is described by a 3d XY model with much narrower critical regime than the NL to SF transition. The size of a supersolid vortex core is much larger than that of a superfluid vortex core. These facts are responsible for the smearing of specific anomaly and the extremely sensitivity to even tiny concentrations of He3 impurities. The SS state is a uniform two-component phase consisting of a normal lattice plus a commensurate superfluid density wave (SDW). The SDW in the SS state leads to a modulation on the X-

ray scattering intensity shifted from that of the NS. The modulation amplitude is proportional to the NCRI observed in the PSU's torsional oscillator experiments. The results achieved in this paper are independent of many microscopic details and should be universal.

Acknowledgement

I am deeply indebted to Tom Lubensky for many insightful and critical comments on the manuscript. I thank P. W. Anderson, T. Clark, M. Cole, D. Huse, J. K. Jain, G. D. Mahan, especially Moses Chan for helpful discussions. The research at KITP was supported by the NSF grant No. PHY99-07949.

-
- [1] A. Andreev and I. Lifshitz, Sov. Phys. JETP **29**, 1107 (1969).
- [2] G. V. Chester, Phys. Rev. A **2**, 256 (1970).
- [3] A. J. Leggett, Phys. Rev. Lett. **25**, 1543 (1970).
- [4] W. M. Saslow, Phys. Rev. Lett. **36**, 1151-1154 (1976).
- [5] E. Kim and M. H. W. Chan, Nature **427**, 225 - 227 (15 Jan 2004).
- [6] E. Kim and M. H. W. Chan, Science **24** September 2004; **305**: 1941-1944.
- [7] D. M. Ceperley, B. Bernu, Phys. Rev. Lett. **93**, 155303 (2004); N. Prokof'ev, B. Svistunov, *ibid.* **94**, 155302 (2005); D. E. Galli, M. Rossi, L. Reatto, Phys. Rev. B **71**, 140506(R) (2005)
- [8] A. T. Dorsey, P. M. Goldbart, J. Toner, cond-mat/0508271. P. W. Anderson, W. F. Brinkman, David A. Huse, Science **18** Nov. 2005; **310**: 1164-1166.
- [9] M. Chan, private communications.
- [10] A. Clark and M. Chan, J. Low Temp. Phys. **138**, 853 (2005).
- [11] A. Clark and M. H. W. Chan, contributed talk at the March meeting, 2005.
- [12] T. Schneider and C. P. Enz, Phys. Rev. Lett. **27**, 1186-1188 (1971); Yves Pomeau and Sergio Rica, Phys. Rev. Lett. **72**, 2426-2429 (1994). P. Nozieres, J. Low. Temp. Phys. **137**, 45 (2004).
- [13] For discussions on Classical Lifshitz Point (CLP) and their applications in nematic to smectic-A and -C transitions in liquid crystal, see the wonderful book by P. M. Chaikin and T. C. Lubensky, principles of condensed matter physics, Cambridge university press, 1995.
- [14] Jinwu Ye, unpublished.
- [15] In real solid He4, $n(x)$ should be a sum of Gaussian instead of a delta function, then $\psi(x=0) \neq 0$, but the qualitative picture stays the same.
- [16] B. A. Fraass, P. R. Granfors, and R. O. Simmons, Phys. Rev. B **39**, 124C131 (1989). C. A. Burns and E. D. Isaacs, Phys. Rev. B **55**, 5767C5771 (1997).
- [17] The precise energy of a vortex in the SDW state will be investigated in a separate publication.